CRYSTAL IMPERFECTIONS WITH REGARD TO DIRECTION IN KAOLINITE MINERAL

D. G. WILLIAMS and C. L. GAREY

The Institute of Paper Chemistry, Appleton, Wisconsin 54911, U.S.A.

Abstract—The crystallite sizes in the particles from four fractions of a kaolinite–clay were determined from the broadening of the X-ray diffraction lines. Measurements were made of the $<002>$ and $<111>$ planes whose crystallographic directions correspond to the clay plate thickness and diagonal, respectively. The extent of crystal imperfection was determined by comparing the calculated crystallite size with the mean size based on measurements from electron micrographs. The crystal imperfections were found to be more extensive in the plate diagonal, $<111>$, than in the plate face, $<002>$, directions. Electron micrographs of hydrofluoric acid-etched samples revealed plate-edge and plate-face imperfections. The latter show a regularity suggesting a mosaic-like texture in the plate surface. Surface imperfections probably have significant influence on the dispersion and flocculation behavior of kaolinite.

INTRODUCTION

It has been generally assumed that dispersants for kaolin clays are adsorbed primarily at the edges of the ideal clay platelets. However, Holtzman (1962) has concluded that anions can be randomly adsorbed over the surface of the kaolinite particle and he suggests that both edge exchange sites and hydrogen bonding to the platelet face are modes of adsorption. Therefore, imperfections in the plate surface could account for adsorption on the plate face.

The creation of stable clay dispersions by specific anion adsorption or by polyelectrolyte adsorption is well documented (Johnson and Norton, 1941), and the behavior of anion stabilized dispersions is described appropriately by the Verwey and Overbeek theory (Verwey and Overbeek, 1948) of hydrophobic colloid stability. If imperfections in the surface of the kaolinite particle could be demonstrated, then it could be concluded that not only are the clay platelets imperfect but also that the adsorption of dispersing agent is not necessarily confined to the exposed edge positions of the clay plate.

In the present study, well-crystallized kaolinite was examined for the extent of crystal imperfections with regard to platelet direction. Fractionated samples of Georgia kaolin clay, which Holtzman (1959) had prepared by sedimentation, were examined by X-ray diffraction line broadening and electron microscopy. The extent of particle imperfection was evaluated by comparing the particle size determined from electron micrographs with the size calculated from diffraction data. Electron micrographs of etched samples revealed the nature of some of the imperfections.

EXPERIMENTAL

Clay fractions

Holtzman (1959) had fractionated a kaolin sample (Engelhard Minerals and Chemicals Corporation, McIntyre, Georgia) by sedimentation and then saturated each of the fractions with hydrogen ions by using an ion-exchange procedure. There were three fractions: $0.2–1.0\ \mu$m effective spherical diameter (ESD), $0.2–0.4\ \mu$m ESD, and $0.4–0.6\ \mu$m ESD, which are designated HF-1, HF-2 and HF-3, respectively. In addition, a new sample of Holtzman's original crude kaolin dispersion (pH = 11, 8 per cent solids) was fractionated by gravity sedimentation to give a large size fraction, $3–9\ \mu$m ESD (A-1). Each of the four dispersions was flocculated by neutralizing with HCl, and then washed with distilled water until a negative $AgNO_3$ test for Cl^- was achieved. The solid fractions were air dried at 50 per cent r.h. and 73°F.

Particle size measurements

Direct measurements of particle size were made from transmission electron micrographs of each fraction. Sample mounts were prepared on copper electron microscope grids and the mounts were then shadowed with palladium at an angle of 30° so that the dimension normal to the grid could be calculated. The electron microscope used was an RCA model EMU-3F.

Each micrograph positive was projected onto a screen so that the horizontal dimension and the shadow length of each particle image could be measured. These values were then converted into actual dimensions of the particles since the magnification factor of

117

the electron micrograph, the projection magnification, and the shadowing angle were known.

The number frequency distribution was converted to a weight percentage distribution. In the case of fraction A-1, both the lengths and widths of the rectangular stacks were measured.

X-ray diffraction measurements

A Norelco (Philips Electronics Corporation) full wave rectified 1 kW X-ray source was used with a copper X-ray tube and nickel filter to give Cu Kα radiation ($\lambda = 1.5418$ Å). A Norelco diffractometer was employed with a Geiger tube detector. The tube was operated such that the counting rate never exceeded about 800 cps, the approximate limit for valid dead time corrections (Klug and Alexander, 1954). The diffractometer slits were 1°, 0·006 in. and 1° for divergence, receiving, and scatter, respectively. Samples were packed into aluminium holders by the method described by Klug and Alexander (1954), but against a frosted glass surface to minimize preferred orientation.

The reference sample for instrumental line broadening was prepared from α-quartz which had been ball milled with stainless steel balls. The steel residue was leached from the powder with aqua regia. After washing, the powder was dispersed in sodium hydroxide (pH = 11) and fractionated by gravity sedimentation to give a 5–20 μm ESD sample. This fraction was then isolated by neutralizing, washing and air drying, as with the clay samples. The material was then annealed at 1120–1150°C (Strong, 1938) for 1 hr and cooled very slowly.

The X-ray diffraction peaks over the range $2\theta = 20$–27°C were examined by manually setting the goniometer angle, 2θ, at selected intervals. The counts were recorded in a fixed time interval, chosen so that the maximum accumulated number was greater than 10,000 counts at the top of the peak, thus assuring < 1 per cent error. Three determinations were made at each setting and the average count rate was used in subsequent calculations. The true count rate, N_o, was calculated from the measured count, N, by (Klug and Alexander, 1954)

$$N = N_o/(1 - K\tau N_o) \qquad (1)$$

where τ is the Geiger tube dead time (1.9×10^{-4} sec as determined from oscilloscopic traces), and K is the statistical factor (1·7 for the full wave rectified source). The profile of the peak was made by plotting N_o vs 2θ and the width at half maximum in degrees 2θ was determined directly from the plot. The α-quartz 101 line ($d = 3.343$ Å, $2\theta = 26.67°$) was used as the instrumental broadening reference for both of the kaolinite

lines examined: 002 ($d = 3.573$ Å, $2\theta = 24.92°$) and 111 ($d = 3.372$ Å, $2\theta = 26.42°$).

The pure line width at half maximum, β, was obtained by using the graphical relationships presented in Klug and Alexander (1954) as follows. The width at half maximum for the reference line, b_o, and for the line to be analyzed, B_o, are corrected for Kα doublet broadening using their Figs. 9–3, Curve B [for line profile intermediate to Gaussian and $1/(1 + k^2\epsilon^2)$], with the separation of the Kα doublet, d, equal to 0·067° at $2\theta = 26°$. Thus, starting with either d/b_o or d/B_o, one obtains b/b_o and B/B_o, where b and B are the respective doublet corrected widths at half maximum. Using their Figs. 9–8 with curves for correcting line breadths for narrow X-ray source instrument broadening [which assumes the instrumental line profile is Gaussian and the pure diffraction line profile is $1/(1 + k^2\epsilon^2)$], the ratio of b/B leads to β/B, from which β can be calculated.

The particle diameter, D, was then calculated from the Scherrer formula:

$$D = \frac{K\lambda}{\beta \cos\theta}$$

where θ is the Bragg angle, λ is the wave length in Å of the X-ray beam used, K is a constant equal to 0·95 for random shaped particles (Klug and Alexander, 1954) and β is expressed in radians.

Clay etching

The clay specimens were etched to reveal surface imperfections by mixing the clay with the desired concentration of hydrofluoric acid solution in a polyethylene container for the desired length of time. A few drops of this slurry were then transferred with the polyethylene stirring rod to 25 ml of distilled water and dispersed. A drop of this dilute dispersion was then used when surface replicas for electron micrographs were prepared.

Electron micrographs of surfaces

Surface replicas of the etched clay samples were prepared in the following manner. A drop of the diluted etched-clay dispersion was placed on a clean microscope slide cover glass and the excess liquid removed slowly with a small piece of filter paper and the specimen then dried. The specimen on the glass was then shadowed at 20° with platinum and then at 90° with carbon to provide a film support for handling. The platinum provides a more uniform surface than palladium, thus giving better surface definition. Next, a softened bead of polystyrene was pressed over the coated specimen and allowed to harden. The glass was then removed leaving the specimen embedded in the plastic.
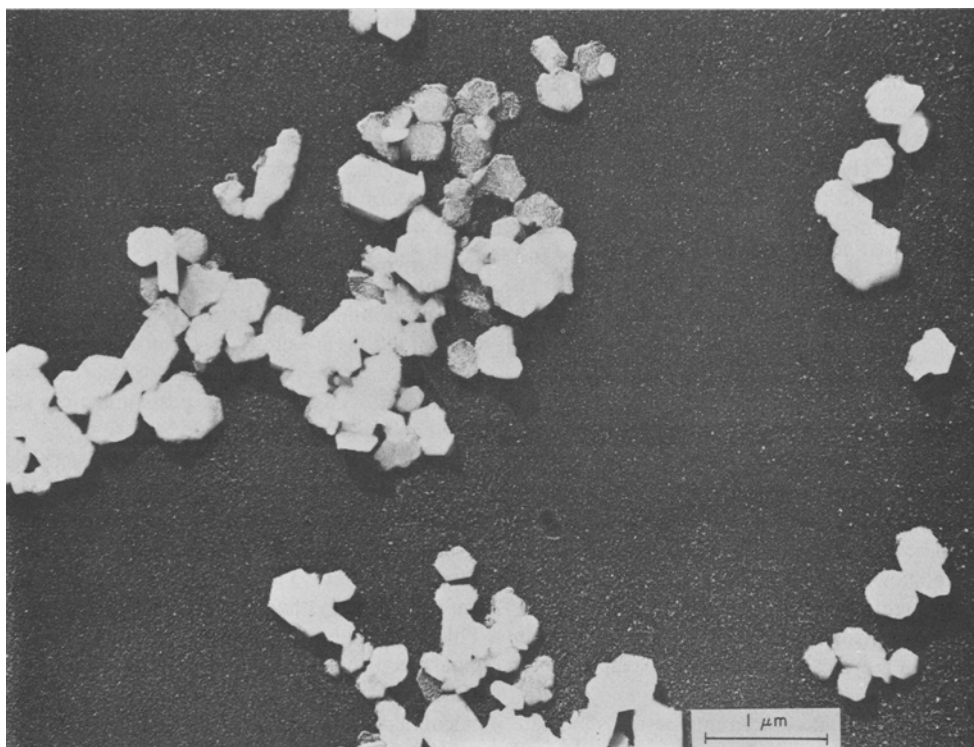
(a)
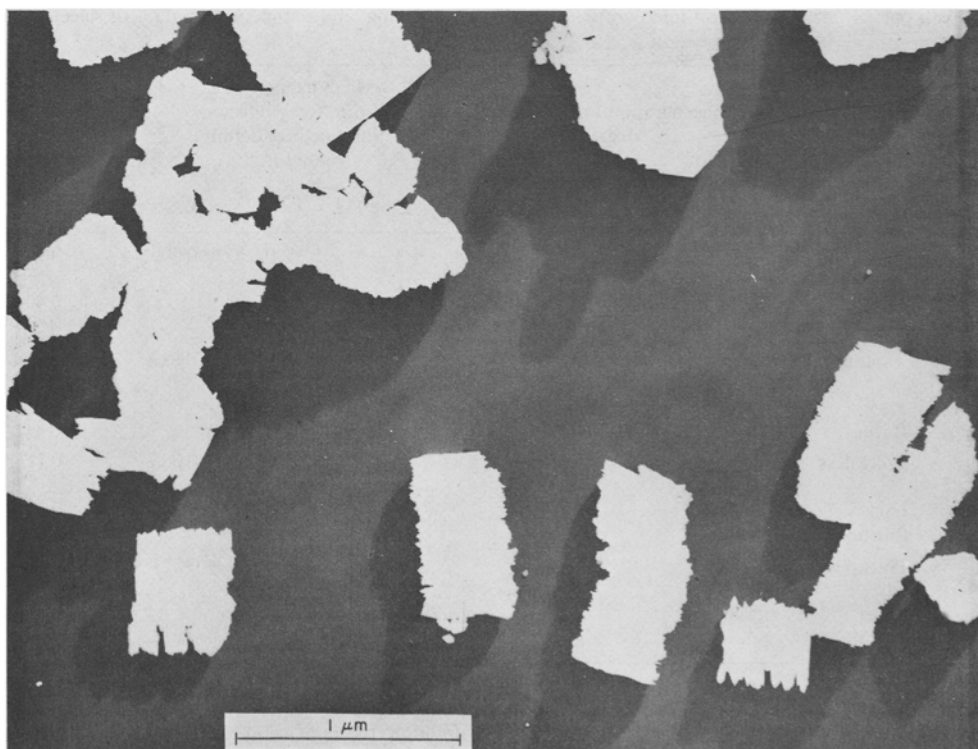
(b)

Fig. 1. Electron micrograph of kaolinite samples shadowed with palladium at 30°: (a) Fraction HF-1; (b) Fraction A-1.

To dissolve the clay away, the polystyrene button was first placed face up on a polyethylene sheet over a steam cone. The exposed clay was covered with a few drops of concentrated HF, making sure that the clay area was wetted at all times. About 1 hr was required for removal of the clay. The polystyrene was then dissolved in benzene and the carbon supported platinum replica placed on an electron microscope grid. Standard electron micrographs of these surface replicas and some stereo-views were prepared.

RESULTS AND DISCUSSION

The electron micrograph of clay fraction HF-1 shown in Fig. 1(a) is representative of the material having a particle size $<1\,\mu$m, revealing the typical hexagonal-shaped plates. Most of the plates lie in a flat position but in some cases the edges can be seen. When the electron beam can penetrate the particle, the edges of some are shown to be tiered or to have steps. An electron micrograph of Fraction A-1 (Fig. 1b) shows particles which consist of stacks of plates viewed on edge. This form is typical of kaolinite particles greater than several micrometers.

Normal X-ray diffraction scanning patterns indicate a small amount of anatase in these clay samples. In all fractions the doublet $11\bar{1}$ and $1\overline{11}$ (4·18 and 4·13 Å, respectively) are partly resolved indicating well-crystallized kaolinite as described by Brindley (1961).

Sedimentation data are on a weight average basis and, therefore, X-ray data comparisons must be made on this basis. The particle dimension distributions for the Fraction HF-1 are shown in Fig. 2. These calculations were made from the number frequency distributions determined from the electron micrographs by weighting each particle according to the cube of the measured dimension. Distribution functions from the other fractions are similar in form. The weight-percentage-based mean particle size for all fractions was obtained directly from such plots and the results are given in Table 1.

The average values obtained from these calculations fall generally within the ESD range of the respective fractions indicating that the ESD is about equivalent to the plate face dimension. The increasing aspect ratio from HF-1 to HF-3 indicates that the particles in HF-3 are more blocky than those in HF-2 and even HF-1. This general impression is also obtained when the original electron micrographs are viewed. The validity of Holtzman's (1963) results are uncertain, because his calculated mean size was based on assumed mathematical models.

Table 1. Mean particle size by electron micrograph, X-ray line broadening, and sedimentation data of selected kaolinite fractions

Sample	Direction relative to plate	Number of particles measured	Mean particle size from plot of weight percentage vs size (μm)	Line 111	Line 002	Holtzman (1962) calculations* (μm)
		Electron micrograph data		Mean particle size from X-ray diffraction line broadening data (μm)		
HF-1 (0·2–1·0 μm)	Thickness	154	0·215	—	0·090 ± 0·002	0·111
	Face	536	0·516	0·081	—	0·404
	Ratio	—	0·417		—	0·274
HF-2 (0·2–0·4 μm)	Thickness	126	0·200	—	0·074 ± 0·017	0·093
	Face	351	0·433	0·052 ± 0·008	—	0·223
	Ratio	—	0·462	—	—	0·418
HF-3 (0·4–0·6 μm)	Thickness	52	0·377	—	0·089 ± 0·006	0·111
	Face	96	0·775	0·041	—	0·365
	Ratio	—	0·486	—	—	0·308
A-1 (3–9 μm)	Thickness†	86	10·7	—	0·136 ± 0·021	—
	Face†	26	3·9	0·028	—	—
	Ratio	—	2·7	—	—	—

* Calculated by the simultaneous solution of the Mueller equation for the equivalent spherical radius of a disk-shaped particle moving with a random orientation in a force field and the equation for specific surface.

† Since only plate stacks lying on their side are found in this fraction, the dimension normal to the specimen surface is equal to the plate face and the dimension parallel to the specimen surface is approximately equivalent to the normal to the plate face.
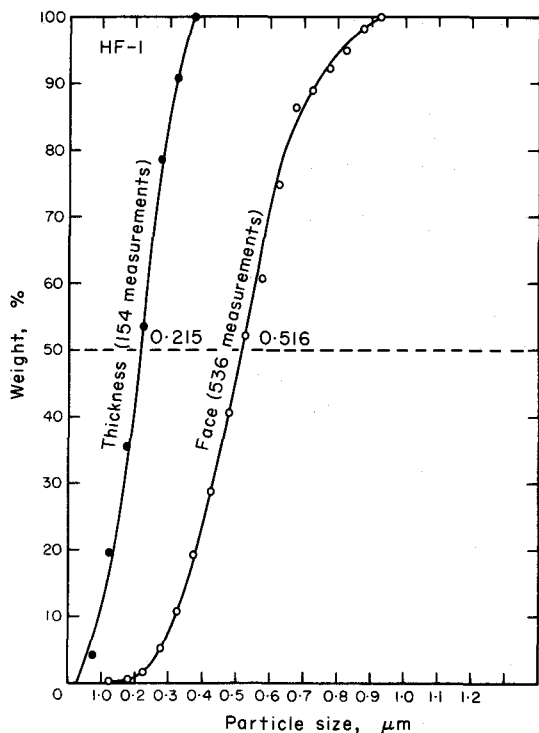
Fig. 2. Particle dimension distribution data from electron micrographs for kaolinite Fraction HF-1.

Fig. 3. X-ray diffraction line profile of kaolinite Fraction HF-1.

The 002 ($d = 3.573$ Å, $2\theta = 24.92°$) and 111 ($d = 3.372$ Å, $2\theta = 26.42°$) diffraction lines were chosen for X-ray line broadening analysis because they represent crystallographic directions normal and diagonal, respectively, to the kaolinite plate. They are similar enough in 2θ to allow the reference line from the α-quartz sample to be used for instrument line broadening corrections. The line broadening of the 111 line represents approximately the imperfections across the plate face because this line contains both a and b axes components. The 101 line ($d = 3.343$ Å, $2\theta = 26.67°$) of the annealed reference sample of α-quartz falls very close to the kaolinite 002 and 111 lines. Using a stable X-ray source, these lines were examined by manually step scanning the same samples several times. Figure 3 is a typical plot of the X-ray diffraction line profile which was obtained for Fraction HF-1 and Fig. 4 is the line profile of the reference sample.

The line widths at half height were converted into equivalent crystallite size by means of the graphical functions and the Scherrer equation as discussed by Klug and Alexander (1954). The results of the line broadening measurements are given in Table 2. The precision and duplication is within ± 3 per cent in the width at half height and within ± 15 per cent in the cal-
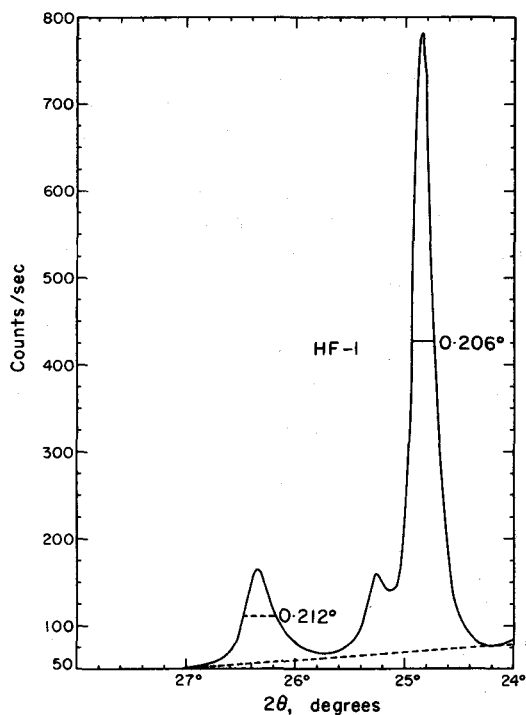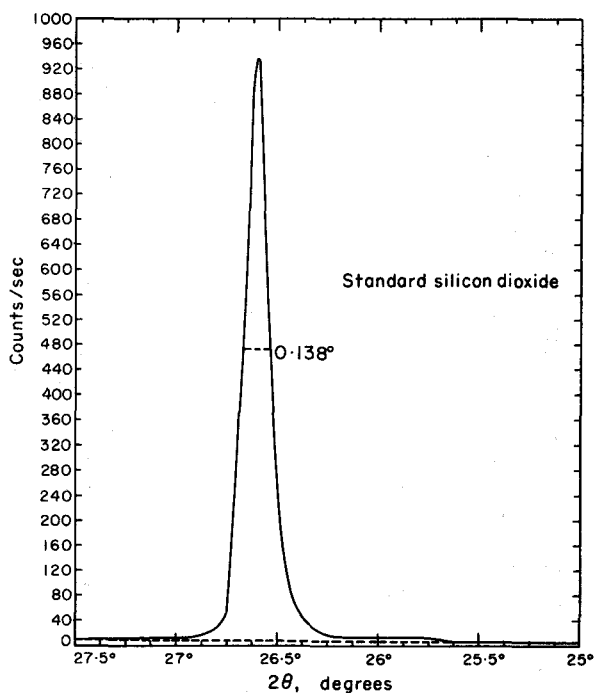

Fig. 4. X-ray diffraction line profile of the silicon dioxide reference sample for instrumental line broadening.

culated particle size. The error for the average of the calculated particles is less than ± 25 per cent, which is reasonably good accuracy. The average of the calculated particle sizes is also listed in Table 1 and may be compared with the measured particle sizes.

For the clay fractions which have definable plate shapes, the average measured plate thickness is two to four times the calculated size indicating that the 002 X-ray diffraction line width includes factors for lattice imperfections other than size. Stacking faults in kaolinite plates would seem to be indicated and perhaps related to the layering evident at many plate edges. For these same fractions, the average size of the measured plate face is 6–20 times the calculated size indicating that the 111 line width was greatly influenced by lattice imperfections. This large lattice imperfection effect in the approximate direction of the plate face is somewhat surprising in view of the smooth appearance of the unetched plates. The data are difficult to reconcile with existing concepts of a planar clay structure. The general trend suggests that the larger the particle, the greater the plate face imperfections.

The above analysis assumes that the clay plate is a single crystal. Attempts were made to verify this by obtaining selected area diffraction patterns of apparent single crystals in this sample. However, the electron beam energy usually caused lattice degradation too quickly for a pattern to be obtained, probably through thermal effects. However, if the plate were to consist of a well-ordered mosaic of smaller crystals, the grain boundaries would constitute imperfections.

Hydrofluoric acid etching of the clay fractions was done in order to bring out the surface imperfections since these points of high free energy should, in general, be places of initial acid attack. Concentrations of 3, 6, 12, 24 and 48 per cent HF were used with etching times of 1, 4 and 16 min at room temperature. Electron micrographs of surface replicas of these were compared to each other and to those from unetched clay. In general, the effects of increasing etching time for constant HF concentration and of increasing HF concentrations for a constant time are about the same.

The plate edges show increased raggedness and the tiers appear to recede to some extent with time or concentration of HF as seen in Fig. 5. Attack at the edges is the more dominant effect and is consistent with selected attack at points of imperfection.

There appeared to be two different modes of attack on the face. One is the development of a roughened surface which increases with time or HF concentration

Table 2. X-ray diffraction line broadening data of selected kaolinite fractions

Sample	Line		Line broadening data*			(Å)
		B_o	0·212°	0·206°		
		β	0·098°	0·094°		
	002	D	882 Å	912 Å		897 $\pm$ 21
HF-1		B_o	—	0·212°		
(0·2–1·0 μm)		β	—	0·105°		
	111	D	—	813 Å		813
		B_o	0·215°	0·224°	0·238°	
		β	0·099°	0·120°	0·136°	
	002	D	871 Å	716 Å	632 Å	740 $\pm$ 171
HF-2		B_o	0·246°	0·262°	0·274°	
(0·2–0·4 μm)		β	0·149°	0·169°	0·183°	
	111	D	581 Å	508 Å	471 Å	520 $\pm$ 79
		B_o	0·205°	0·211°		
		β	0·092°	0·101°		
	002	D	937 Å	849 Å		893 $\pm$ 62
HF-3		B_o	—	0·293°		
(0·4–0·6 μm)		β	—	0·209°		
	111	D		412 Å		412
		B_o	0·188°	0·176°		
		β	0·071°	0·057°		
	002	D	1210 Å	1505 Å		1358 $\pm$ 209
A-1		B_o	—	0·376°		
(3–9 μm)		β	—	0·305°		
	111	D	—	278 Å		278

* The 101 line ($2\theta = 26·67°$) of α-quartz (3–9 μm, annealed) is the instrument broadening reference with a measured width at half maximum, $b_o = 0·138°$, and a doublet separation, $d = 0·067°$ at $2\theta = 26·00°$, for a corrected width, $b = 0·101°$. The symbols B_o, β and D are the measured width at half maximum, the width at half maximum of the pure diffraction line, and the particle size calculated from the Scherrer equation, respectively.
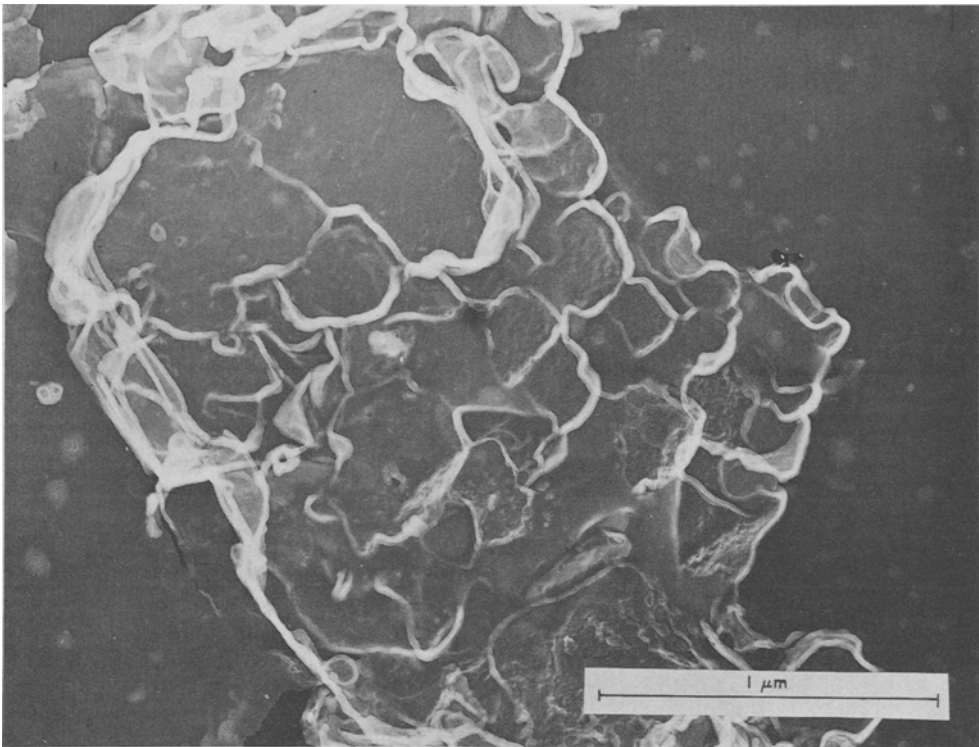
Fig. 5. Electron micrograph of a surface replica of kaolinite Fraction HF-1 etched 1 min in 6 per cent HF showing both plate edge and face attack with the development of bumpiness.
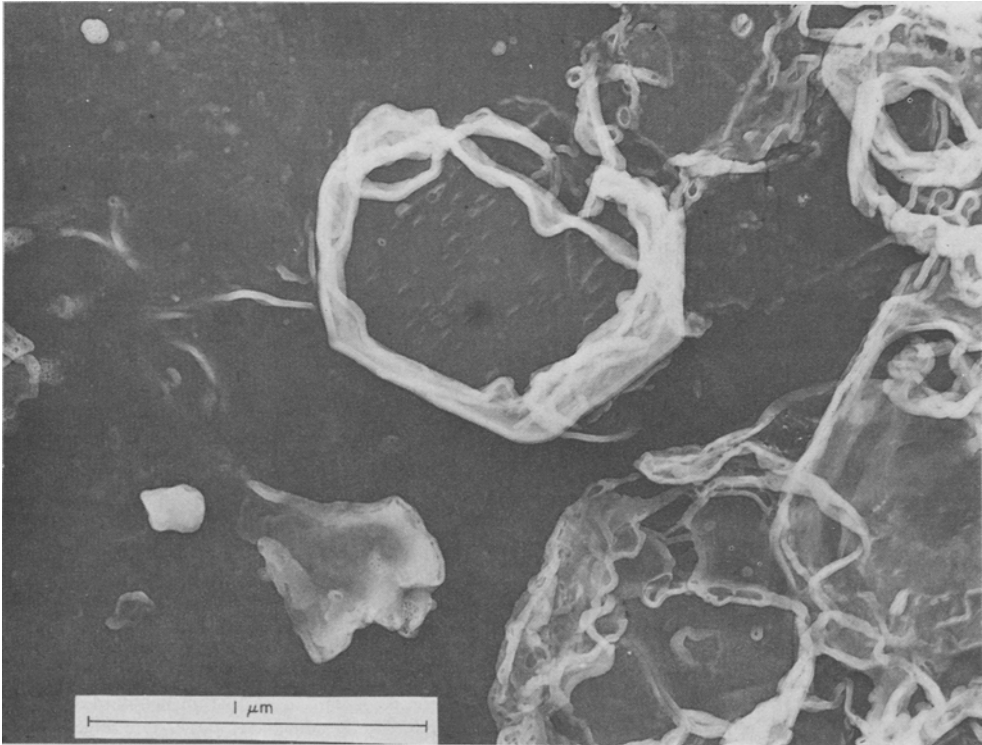

Fig. 6. Electron micrograph of a surface replica of kaolinite Fraction HF-1 etched 1 min in 6 per cent HF showing plate face attack with the development of parallel crevices.

123

(see the particles in the central region of Fig. 5). Stereo-views of electron micrographs revealed that this rough-ness was in a cavernous indentation in the face of the particle. The other mode is the development, on a generally smooth surface, of parallel crevices which lengthen and widen with time or HF concentration (see Fig. 6). Some of these slots are part of triangular cracks as at the corner of three hexagons. These cre-vices are definite evidence of plate surface imperfec-tions and their common direction is indicative of boundaries in a crystalline mosaic.

The X-ray line broadening data and the electron micrographs indicate that lattice imperfections are a significant part of crystalline kaolinite. The imperfec-tions at the surface should be good adsorption sites for ions or polymer segments in the dispersion or floccula-tion processes. Thus, the distribution of adsorbed spe-cies should be at least as frequent on the plate face as on the edge and the effect of particle geometry and idealized structure on dispersion and flocculation should be limited.

CONCLUSIONS

The crystal imperfections in good crystalline kao-linite are more extensive in the hexagonal-plate dia-gonal, $<111>$, than in the plate thickness, $<002>$. Thus, surface imperfections may also be common on the plate face. Hydrofluoric acid-etch indicates the pres-ence of both plate edge and face imperfections, the lat-ter in some cases indicating a mosaic-like structure of the plate. Adsorption sites related to surface imperfec-tion should be as common on the kaolinite plate face as on the edge and should be a factor in dispersion of kaolinite clays.

REFERENCES

Brindley, G. W. (1961) *The X-Ray Identification and Crystal Structures of Clay Minerals*, (Edited by Brown, G.), Chap. II. Mineralogical Society, London.

Holtzman, W. (1959) *The Application of the Verwey and Overbeek Theory of the Stability of Kaolinite–Water Sys-tems*. Doctors Dissertation. The Institute of Paper Che-mistry, Appleton, Wis.

Holtzman, W. (1962) *J. Coll. Sci.* **17**, 363–382.

Johnson, A. L. and Norton, F. A. (1941) *J. Am. Ceram. Soc.* **24**, 189.

Klug, H. P. and Alexander, L. E. (1954) *X-Ray Diffraction Procedures for Polycrystalline and Amorphous Materials*, p. 716. Wiley, New York.

Strong, J. (1938) *Procedures in Experimental Physics*: p. 642. Prentice-Hall, New Jersey.

Verwey, E. J. W. and Overbeek, J. T. G. (1948) *Theory of the Stability of Lyophobic Colloids*, p. 206, Elsevier, New York.

Résumé—La taille des cristallites dans les particules provenant de quatre fractions d'une kaolinite a été déterminée par l'élargissement des pics de diffraction X. Les mesures ont été effectuées pour les plans $\langle 002 \rangle$ et $\langle 111 \rangle$ dont les directions cristallographiques correspondent respectivement à l'épaisseur et à la dia-gonale de la plaquette d'argile. Le degré d'imperfection cristalline a été déterminé en comparant la taille calculée à la taille moyenne basée sur les mesures faites à partir des micrographies électroniques. On a trouvé que les imperfections cristallines sont plus importantes dans la direction $\langle 111 \rangle$ de la diagonale de la plaquette, que dans la direction $\langle 002 \rangle$ de sa surface. Les micrographies électroniques d'échantillons attaqués à l'acide fluorhydrique révèlent des imperfections sur les bords et les faces des plaquettes. Ces dernières montrent une régularité qui suggère, à la surface, une texture mosaïque. Les imperfections de surface ont probablement une influence notable sur le comportement de la kaolinite à la dispersion et à la floculation.

Kurzreferat—Die Kristallitgrößen in Teilchen aus vier Fraktionen eines Kaolinittones wurden aus der Verbreiterung der Röntgenbeugungslinien bestimmt. Die Messungen wurden an den $\langle 002 \rangle$- und $\langle 111 \rangle$-Ebenen durchgeführt, deren kristallographische Richtung der Tonplättchendicke bzw. der Diagonalen entspricht. Das Ausmaß der Gitterfehlordnungen wurde durch einen Vergleich der berechneten Kristal-litgröße mit der auf Grund von Messungen an elektronenmikroskopischen Aufnahmen ermittelten Größe errechnet. Die Gitterfehler erwiesen sich als ausgeprägter in Richtung der Teilchendiagonalen $\langle 111 \rangle$ als in Richtung senkrecht zur Teilchenebene $\langle 002 \rangle$. Elektronenmikroskopische Aufnahmen mit Flußsäure angeätzter Proben wiesen Baufehler an den Plattenkanten und den Plattenflächen auf. Letztere zeigen eine Regelmäßigkeit, die auf mosaikartige Strukturen an Plättchenoberflächen hindeutet. Oberflächendefekte haben wahrscheinlich einen bedeutenden Einfluß auf das Dispersions- und Flockungsverhalten des Kao-linits.

Резюме — По уширению линий на рентгенограмме опряделяли размеры кристаллитов в частицах четырех обломков каолинитовой глины. Измеряли плоскости $\langle 002 \rangle$ и $\langle 111 \rangle$, кристаллографические направления которых соответствовали толщине и диагонали глинистой пластинки, соответственно. Дефекты кристаллов определяли сравнением высчитанного размера кристаллита со средним размером, базированном на измерениях с электронномикроскопических снимков. По диагональному $\langle 111 \rangle$ направлению пластинки нашли больше дефектов в кристаллах, чем по поверхностному $\langle 002 \rangle$ направлению пластинки. Электронномикроскопические снимки и образцы протравленные фтористоводородной кислотой выявили краевые и поверхностные дефекты. Последные распределены так регулярно, что предполагают, что текстура поверхности пластинки является мозаичной. Дефекты поверхности, вероятно, заметно влияют на поведение распространения и флоккулирования каолинита.